State selective electron capture in collisions of ground and metastable O^{2+} ions with H(1s).

C. N. Cabello[†], L. F. Errea[†], L. Fernández[†], L. Méndez[†], A. Macías[†,‡], I. Rabadán[§†] and A. Riera[†]

[†] Departamento de Química, Universidad Autónoma de Madrid, Madrid-28049, Spain
[‡] Instituto de Estructura de la Materia, CSIC, Serrano 123, Madrid-28006, Spain

Abstract. An *ab initio* calculation of the electron capture cross sections for collisions of ground and metastable states of O^{2+} with H(1s) is presented. For impact energies between 0.125 and 3.4 keV/amu, we find good agreement between the cross sections from the ground state ion with the mixed beam experimental data of Phaneuf *et al* (1982).

PACS numbers: 34.70.+e, 34.10.+x

1. Introduction

Electron capture (EC) in ion–atom(molecule) collisions are important processes in astrophysical and fusion plasmas. However, the measurement of cross sections for these processes is often difficult due to the presence of unknown quantities of metastable species in the ion beam. Examples of this difficulty are C^{2+} collisions with H, He, and H_2, which have been considered in several theoretical and experimental works (Unterreiter *et al* 1991, Castillo *et al* 1994, Leputsch *et al* 1997, Voulot *et al* 2000, Errea *et al* 2000*a*, Errea *et al* 2000*b*). Recently, double translational energy techniques have allowed to measure EC cross sections for ions in both ground and metastable states (see, e.g. the data for $C^{2+} + H$ and $N^{2+} + H$ collisions of Voulot *et al* (2000) and Voulot *et al* (2001)). Similarly, O^{2+} beams from usual ion sources are, in principle, a mixture of unknown proportions of ground state ($1s^2 2s^2 2p^2\ ^3P$) and metastable ($1s^2 2s^2 2p^2\ ^1D$ and $1s^2 2s^2 2p^2\ ^1S$) ions, and accordingly, the following EC reactions can take place in $O^{2+} + H$ experiments:

$$O^{2+}(1s^2 2s^2 2p^2\ ^3P) + H(1s) \rightarrow O^+ + H^+ \quad (1)$$

$$O^{2+}(1s^2 2s^2 2p^2\ ^1D) + H(1s) \rightarrow O^+ + H^+ \quad (2)$$

$$O^{2+}(1s^2 2s^2 2p^2\ ^1S) + H(1s) \rightarrow O^+ + H^+ \quad (3)$$

Experimental works on this system include the measurements of EC cross sections of Phaneuf *et al* (1982), carried out with a mixed beam. McLaughlin *et al* (1990) measured

§ To whom correspondence should be addressed (Ismanuel.Rabadan@uam.es)

EC energy change spectra for impact energies in the range 0.125–0.5 keV/amu using also a mixed beam; the recorded spectra show two peaks, one at $\Delta E \simeq 6.5$ eV and a second at 3.5 eV; this second peak was assigned to capture by metastable ions. The use of double translational energy spectroscopy technique allowed to record the energy change spectrum for EC at a collision energy of 0.375 keV/amu and for an incident pure beam of ground state ions (McCullough 2000), which showed a single peak at $\Delta E \simeq 6.5$ eV corresponding to EC into $O^+(1s^2 2s 2p^4\ ^4P)$. EC cross sections have not been measured with pure beams and state selective experimental cross sections have not been reported hitherto.

From the theoretical point of view, the calculation of EC cross sections at low impact energies is carried out by employing a molecular expansion, which involves the previous evaluation of potential energy surfaces and dynamical couplings of the corresponding quasimolecule. For many-electron systems, this calculation requires the adaptation of quantum chemistry packages. In particular, for collisions involving metastable species, several initial states must be considered, and one has to include a relatively large number of molecular states, which must be evaluated with the same precision in a wide range of internuclear separations; this is a non standard task for those packages, and their application to dynamical problems have been considered in previous works (Castillo *et al* 1994, Castillo *et al* 1995, Errea *et al* 2000*b*).

Honvault *et al* (1994) evaluated total cross sections for reactions (1–3) at a range of energies from 1.25 eV/amu to 1.87 keV/amu. The molecular energy curves and couplings were evaluated by using a SCF-CI technique, where the ground state is, in general, described more precisely than the excited states. The results from that calculation suggested that a relatively high proportion (60%) of metastable ions was present in the experiment of Phaneuf *et al* (1982). Given the sensitivity of the cross sections to the quality of the molecular data, and in order to evaluate state-selective EC cross sections, we have carried out an extensive molecular calculation using the techniques previously applied to C^{2+}+H,H_2 collisions (Errea *et al* 1999, Errea *et al* 2000*b*, Errea *et al* 2000*a*).

Our dynamical calculations have been carried out by applying a method similar to that of Errea *et al* (2000*a*), which is described in section 2. We employ a semiclassical treatment with a close-coupling molecular expansion, where the electronic energies and non-adiabatic couplings for doublet and quadruplet states of the OH^{2+} quasimolecule are obtained in a multireference configuration interaction calculation. The details of the molecular calculation are presented in section 3 and the dynamical calculations in section 4. Our main conclusions are outlined in section 5. Atomic units are used unless otherwise indicated.

2. Method

For not too low impact energies ($E \gtrsim 50$ eV/amu), the dynamics of ion-atom collisions is usually treated using the impact-parameter method (see e.g. Bransden and McDowell (1992)), where the nuclear motion follows straight-line trajectories with constant velocity

$\boldsymbol{v}$ and impact parameter $\boldsymbol{b}$ ($\boldsymbol{R} = \boldsymbol{b} + \boldsymbol{v}t$), while the electronic motion is described by the wavefunction $\Psi(\boldsymbol{r}, t; b, v)$, solution of the equation

$$\left(H_{\rm elec} - \mathrm{i}\frac{\partial}{\partial t}\bigg|_{\boldsymbol{r}} \right) \Psi(\boldsymbol{r}, t; b, v) = 0 \tag{4}$$

where $H_{\rm elec}(\boldsymbol{r}; R)$ is the non-relativistic, clamped-nuclei Born-Oppenheimer electronic Hamiltonian, and $\boldsymbol{r}$ denotes the electronic coordinates. If n_A and n_B are the number of electrons initially attached to nucleus A and B, respectively, the semiclassical equation (4) must be solved with the initial condition:

$$\Psi(\boldsymbol{r}, t; b, v) \underset{t \to -\infty}{\sim} \Phi_i^A \Phi_i^B \prod_{j=1}^{n_A} D^A(\boldsymbol{r}_j) \prod_{j'=1}^{n_B} D^B(\boldsymbol{r}_{n_A+j'}) \times \exp\left[-\mathrm{i}(E_i^A + E_i^B)t\right] , \tag{5}$$

where $\Phi_i^{A,B}$ are atomic wavefunctions with energies $E_i^{A,B}$, and $D^{A,B}$ are plane-wave translation factors, which describe the translation motion of the electrons attached to each nucleus:

$$D^X(\boldsymbol{r}_j) = \exp\left[-\mathrm{i}(\boldsymbol{v}_X \cdot \boldsymbol{r}_j + \frac{1}{2} v_X^2 t)\right] \; ; \;\; (X = A,\ B) \tag{6}$$

where $\boldsymbol{v}_{A,B}$ are the nuclear velocities with respect to the electronic coordinates origin, placed at an arbitrary point of the internuclear axis.

Analogously to equation (5), the wavefunction for a collisional final state is:

$$\psi_f(\boldsymbol{r}, t; b, v) = \Phi_f^A \Phi_f^B \prod_{j=1}^{n'_A} D^A(r_j) \prod_{j'=1}^{n'_B} D^B(r_{n'_A+j'}) \times \exp\left[-\mathrm{i}(E_f^A + E_f^B + \alpha_f)t\right] , \tag{7}$$

where $|n'_A - n_A|$ is the number of electrons that have been exchanged and $\alpha_f = Q_A Q_B v^{-1} \log(R - vt)$ comes from the Coulomb interaction between the two ions with charges $Q_{A,B}$ formed in the collision.

To solve equation (4), Ψ is expanded in a set of (approximate) eigenfunctions ϕ_k of $H_{\rm elec}$:

$$\Psi(\boldsymbol{r}, t; b, v) = \exp(\mathrm{i}U) \sum_k a_k(t; b, v) \phi_k(\boldsymbol{r}; R) \exp\left(-\mathrm{i}\int_{-\infty}^{t} \epsilon_k \mathrm{d}t'\right) \tag{8}$$

where

$$H_{\rm elec}(\boldsymbol{r}; R)\phi_k(\boldsymbol{r}; R) = \epsilon_k(R)\phi_k(\boldsymbol{r}; R) \tag{9}$$

and $\exp[\mathrm{i}U(\boldsymbol{r}, t)]$ is a common translation factor (Schneiderman and Russek 1969). Our translation factor has the form (see Errea *et al* (1994)):

$$U(\boldsymbol{r}, t) = \sum_{j=1}^{n_A+n_B} \left[f(\boldsymbol{r}_j, R)\boldsymbol{v} \cdot \boldsymbol{r}_j - \frac{1}{2} f^2(\boldsymbol{r}_j, R) v^2 t \right] \tag{10}$$

with (Errea *et al* 1982):

$$f(\boldsymbol{r}_j, R) = g(R)\, \boldsymbol{r}_j \cdot \widehat{R} = \frac{R}{R^2 + \beta^2}\, \boldsymbol{r}_j \cdot \widehat{R}\,. \tag{11}$$

In the present calculation, the switching function f has been defined with $\beta = 2$ and with the coordinates $\boldsymbol{r}_j$ referred to the O nucleus. Substitution of equation (8) in (4) leads to the system of differential equations:

$$\mathrm{i}\dot{a}_k = \sum_l M_{kl} a_l \exp\left[-\mathrm{i}\int_{-\infty}^{t} (\epsilon_l - \epsilon_k)\mathrm{d}t'\right], \tag{12}$$

where $M_{kl}(R; b, v)$ are the non-adiabatic couplings:

$$M_{kl} = \left\langle \exp(\mathrm{i}U)\phi_k \left| H_{\mathrm{elec}} - \mathrm{i}\frac{\partial}{\partial t}\right| \exp(\mathrm{i}U)\phi_l \right\rangle \tag{13}$$

In the energy range of this work, the transitions between the molecular states are mainly due to the components of M_{kl} proportional to v, which have the form:

$$\frac{v^2 t}{R} R_{kl} + \frac{bv}{R^2} L_{kl} \tag{14}$$

and, by analogy with the molecular expansion without translation factors, R_{kl} and L_{kl} are known as modified radial and rotational couplings, respectively. For the translation factor of equations (10) and (11), they are:

$$R_{kl} = \left\langle \phi_k \left| \frac{\partial}{\partial R} + \sum_j \left[(Rg^2 - 2g)\, z_j \frac{\partial}{\partial z_j}\right] \right| \phi_l \right\rangle \tag{15}$$

and

$$L_{kl} = \left\langle \phi_k \left| \sum_j \left[\mathrm{i}L_y(\boldsymbol{r}_j) - gR\left(x_j \frac{\partial}{\partial z_j} + z_j \frac{\partial}{\partial z_j}\right)\right] \right| \phi_l \right\rangle \tag{16}$$

where L_y is the Y component of the electronic angular momentum operator, and x_j, z_j are the electronic coordinates in the molecular reference frame.

The probability for transition to the final state ψ_f is calculated from the coefficient a_f of equation (8)

$$P_f(b, v) = \lim_{t\to\infty} |\langle \psi_f | \Psi\rangle - \delta_{if}|^2 = \lim_{t\to\infty} |a_f(t; b, v) - \delta_{if}|^2 \ , \tag{17}$$

and the total cross section for transition to this state is:

$$\sigma_f(v) = 2\pi \int_0^\infty b P_f(b, v)\, \mathrm{d}b\,. \tag{18}$$

3. Molecular calculations

Since the entrance channel of reaction (1) correlates to quadruplet and doublet molecular states, and those of reactions (2) and (3) correlate with doublet states, we have calculated doublet and quadruplet states of the OH^{2+} quasimolecule.

The molecular states ϕ_j and energies ϵ_j were obtained by using a multireference configuration interaction method (MRCI) with the program MELD (Davidson 1990). This method involves, in a first step, a SCF calculation in a basis of Gaussian type orbitals (GTOs), which provides a set of molecular orbitals (MOs). A set of reference

configurations is then selected. Each reference configuration is a symmetry- and spin-adapted linear combination of a few Slater determinants built up from products of the MOs. The configuration interaction (CI) space includes single and double excitations from the reference set.

In the present calculation, the GTO basis sets, centered at the O and H nuclei, were taken from Widmark *et al* (1990) and consist in {4s,3p,2d} and {3s,2p} contracted GTOs, respectively. The MOs were obtained in a restricted SCF calculation of the OH^{5+} system. In this case, in the limit $R \to \infty$, the SCF configuration correlates to the $1s^2 2s^2$ configuration of O^{4+}, so the $2p_x$ and $2p_y$ orbitals, both unoccupied, have the same coefficients. This allows to describe, with the same accuracy, the states involved in the collisional system (see table 1). We have checked that the calculated molecular energies do not significantly change when the CI calculation is carried out with MOs obtained in a SCF calculation for the OH^{7+} quasimolecule. The CI space was built from a set of 160 reference configurations, but, to obtain a reasonable size of this space, we have introduced the following restrictions: i) Frozen core approximation, which means that we keep only configurations with the ground MO, 1σ, doubly occupied. ii) Second order perturbation theory is used to select doubly excited configurations. In this selection, our zeroth order wavefunctions are the eigenvectors of the Hamiltonian matrix in the basis of reference configurations, and we have included configurations with a contribution to the energy of the first 18 quadruplet and 27 doublet states greater than 5×10^{-6} Hartree.

The set of reference configurations was selected iteratively at each R in the following way: An initial guess of 160 reference configurations was generated in the limit $R \to \infty$, which contained the basic structures of the atomic channels to be included in the dynamical calculation (those listed in table 1). Using this set we carried out a MRCI calculation, and we selected the 160 configurations with the largest contributions to the lowest 18 (quadruplets) and 27 (doublets) states obtained in this calculation, which were then used as a new reference set and the selection procedure was repeated. After three iterations the reference set has converged and the weight of the reference configurations in the calculated CI functions is larger than 95% for the states of table 1. To ensure a similar precision of wavefunctions at any internuclear distance, the selection of the reference set was repeated at each value of R, with the converged reference set at a given value of the internuclear distance, R_i, used as the initial guess in a nearby point R_{i+1} ($R_i > R_{i+1}$). In practice, $R_i - R_{i+1} = 0.2$ a_o except for $R < 4$ a_o and in the region of avoided crossings at 8.5–9.3 a_o, where the stepsize was reduced to 0.05 a_o. The CI space included about 20000 Slater determinants for each multiplicity, while the calculation of Honvault *et al* (1994) included less than 400.

As a check of the accuracy of our calculation, we compare in table 1 the calculated energies of the O^+ and O^{2+} states included in the dynamical calculation with the experimental values of Moore (1971). The tabulated energies are relative to the ground state of O^{2+}. The errors in these energy differences are smaller than 0.5 eV for the relevant channels, sufficient for the dynamical calculation. Also included in the table are the corresponding molecular states of OH^{2+}.

Table 1. Comparison of O^+, O^{2+} energy differences ($E_i - E_1$) (in eV) with experimental ones (Moore 1971). Also, the molecular states (MS) of the OH^{2+} quasi-molecule to which the atomic states correlate.

i	Channel	This work	(Moore 1971)	M.S.
1	$O^{2+}(2s^22p^2\ ^3P)$	0.000	0.000	$^{2,4}\Pi$, $^{2,4}\Sigma^-$
2	$O^{2+}(2s^22p^2\ ^1D)$	2.718	2.514	$^2\Sigma^+$, $^2\Pi$, $^2\Delta$
3	$O^{2+}(2s^22p^2\ ^1S)$	5.570	5.355	$^2\Sigma^+$
4	$O^{2+}(2s2p^3\ ^5S^\circ)$	7.178	7.480	$^4\Sigma^-$
5	$O^{+}(2s2p^4\ ^4P)$	−20.006	−20.289	$^4\Pi$, $^4\Sigma^-$
6	$O^{+}(2s2p^4\ ^2D)$	−13.995	−14.566	$^2\Sigma^+$, $^2\Pi$, $^2\Delta$
7	$O^{+}(2s^22p^23s\ ^4P)$	−12.093	−12.180	$^4\Pi$, $^4\Sigma^-$
8	$O^{+}(2s^22p^23s\ ^2P)$	−11.568	−11.728	$^2\Pi$, $^2\Sigma^-$
9	$O^{+}(2s2p^4\ ^2S)$	−10.218	−10.857	$^2\Sigma^+$
10	$O^{+}(2s^22p^23p\ ^2S^\circ)$	−9.464	−9.861	$^2\Sigma^-$

In figures 1 and 2 we plot the potential energy curves for the molecular states dissociating into O^{2+}+H(1s) and O^++H^+, with O^+ and O^{2+} in the states of table 1, and where the molecular states are labeled according to their asymptotic limits of table 1. The entrance channels for reaction (1) are the molecular states $1^4\Sigma^-$, $1^4\Pi$, $1^2\Sigma^-$ and $1^2\Pi$; the entrance channels for reaction (2) are $2^2\Sigma^+$, $2^2\Pi$ and $2^2\Delta$; and $3^2\Sigma^+$ is the entrance channel for reaction (3).

The dynamical couplings of equation (13) were evaluated numerically as explained in Castillo *et al* (1995); this method involves the calculation of the delayed overlap matrix elements $< \phi_i(\boldsymbol{R}) \mid \phi_j(\boldsymbol{R}+\boldsymbol{\delta}) >$. In this work we have used $|\boldsymbol{\delta}| = 10^{-4}$ a_o. An important practical difficulty in applying the molecular expansion to many-electron systems is the erratic sign of the approximate eigenfunctions ϕ_i, which results in meaningless signs of the dynamical couplings. To solve this arbitrariness, we have implemented an algorithm to automate the sign coherence of the molecular states ϕ_i, both between successive grid points ($\boldsymbol{R}_j$, $\boldsymbol{R}_{j+1}$) and the calculation of the couplings ($\boldsymbol{R}_j$, $\boldsymbol{R}_j+\boldsymbol{\delta}$). This method is based on the evaluation of the delay overlaps $< \phi_i(\boldsymbol{R}) \mid \phi_i(\boldsymbol{R}+\boldsymbol{\delta}) >$ and $< \phi_i(\boldsymbol{R}_j) \mid \phi_i(\boldsymbol{R}_{j+1}) >$.

As an illustration, we have plotted in figure 3 the most important modified radial couplings (see equation (15)) and in figure 4 some rotational ones (equation (16)). The main mechanism of reaction (1) involves transitions in the neighborhood of $1^4\Sigma^-$–$5^4\Sigma^-$ (at $R \simeq 4.0$ and 3.5 a_o) and $1^4\Pi$–$5^4\Pi$ (at $R \simeq 4.5$ and 2.5 a_o) avoided crossings in figure 1, which are responsible for the two-peak structure of the corresponding couplings in figure 3a. These transitions are strongly modified by the rotational transitions induced by $1^4\Sigma$–$1^4\Pi$ and $5^4\Sigma$–$5^4\Pi$ rotational couplings of figure 4a.

Reaction (2) takes place through transitions between states of the multiplets 2 (the entrance channels) and 6 in the avoided crossings at R in the range 2–3 a_o (see figure 3b). Also, in the range of impact energies of this work, small transitions take place in the sharp avoided crossings at $R \simeq 8.8$ a_o (figure 3c), which are crossed almost diabatically.

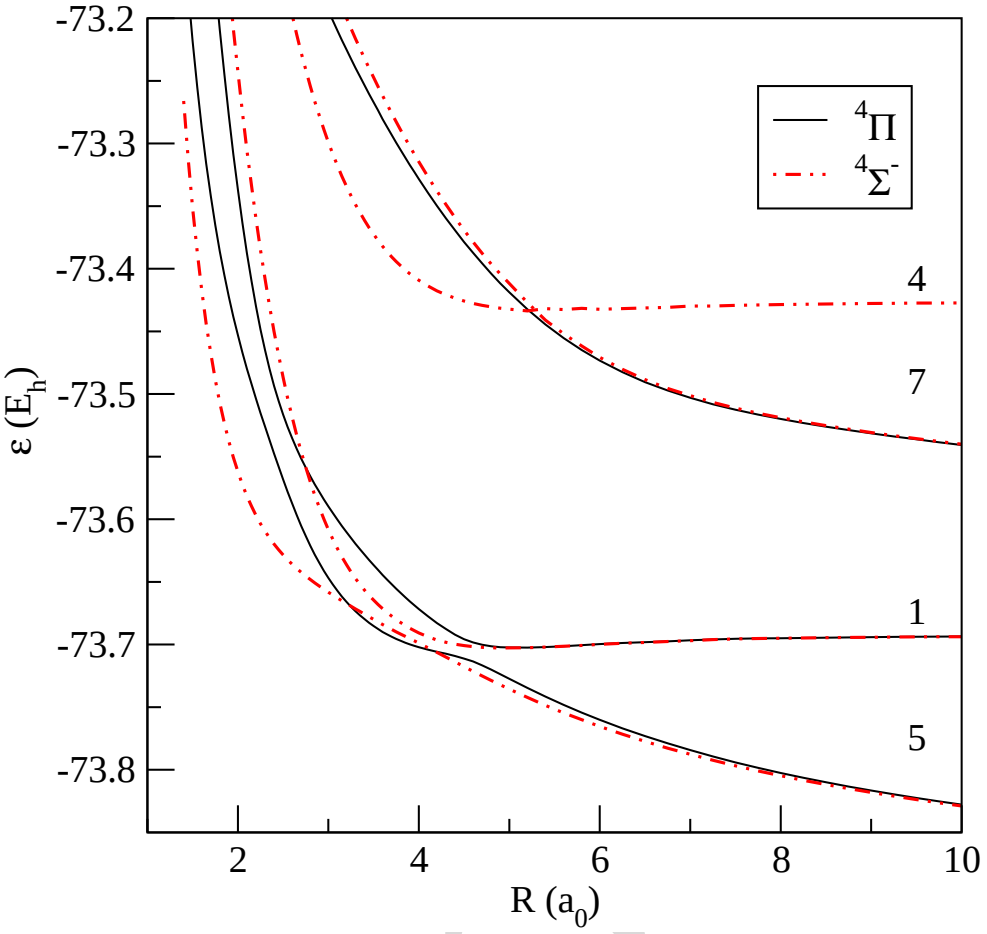

Figure 1. Potential energy curves for the OH^{2+} quadruplets subsystem. Channels are labeled according to table 1.

However, these transitions cannot be neglected in the calculation of cross sections for reaction (2) because of the large internuclear distances involved. The energy of the molecular state $3^2\Sigma^+$, which is the entrance channel of reaction (3), shows avoideded crossings with that of state $2^2\Sigma^+$ at $R \simeq 4.8$ and 2.5 a_o. The most important transitions leading to reaction (3) are due to the radial couplings between the entrance channel and states 2 and $9^2\Sigma^+$ plotted in figure 3d.

4. Results

Our calculated total cross sections for reactions (1)–(3) are listed in table 2 and plotted in figure 5, where we have also included the contribution of the quadruplets states to the cross section of reaction (1) to show that this process is dominated by the quadruplet subsystem. In figure 6, we plot the contribution ratio of the individual channels, calculated as

$$k_i = \frac{\sigma_i}{\sum_j \sigma_j}\,, \tag{19}$$

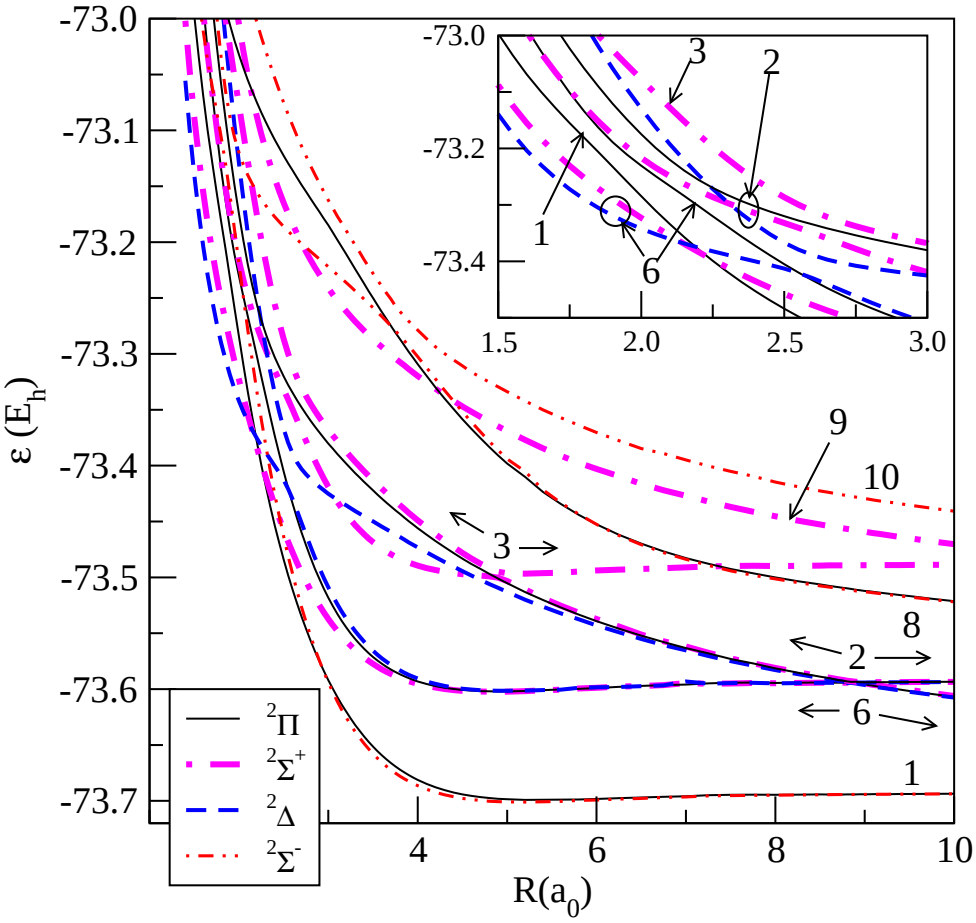

Figure 2. Potential energy curves for the OH^{2+} doublets subsystem. Channels are labeled according to table 1. The inset contains only states of channels 1, 2, 3 and 6 of symmeties $^2\Sigma^+$, $^2\Pi$ and $^2\Delta$.

with i and j running over the EC channel index.

At low energies (below 1.25 keV/amu), the EC process (1) involves the capture of the target electron into the 2p orbital with simultaneous excitation of a 2s electron to the 2p orbital (exit channels 5 and 6 of table 1). This result agrees with the translation energy spectra of McLaughlin *et al* (1990) and McCullough (2000) which exhibit a single peak for reaction (1) at $E < 0.5$ keV/amu. At higher energies, the capture into the 3s orbital (channels 7 and 8) becomes competitive with the previous process, and these transitions are responsible for the increase of the total cross section in figure 5 for $E > 1.25$ keV/amu.

Reaction (2) takes place through transitions in the avoided crossings $2^2\Sigma^+$–$6^2\Sigma^+$, $2^2\Pi$–$6^2\Pi$ and $2^2\Delta$–$6^2\Delta$, which explains that $O^+(^2D)$ is the most abundant product of this reaction. $O^+(^2S)$ is a secondary output of this process with a contribution rising up to 10% at 1.25 keV/amu (see figure 6); this channel is populated through a two-step mechanism $6^2\Sigma$–$3^2\Sigma$–$9^2\Sigma$. Again, our results are consistent with translation energy spectra of McLaughlin *et al* (1990), which show a second peak at $\Delta E \simeq 3.4$ eV

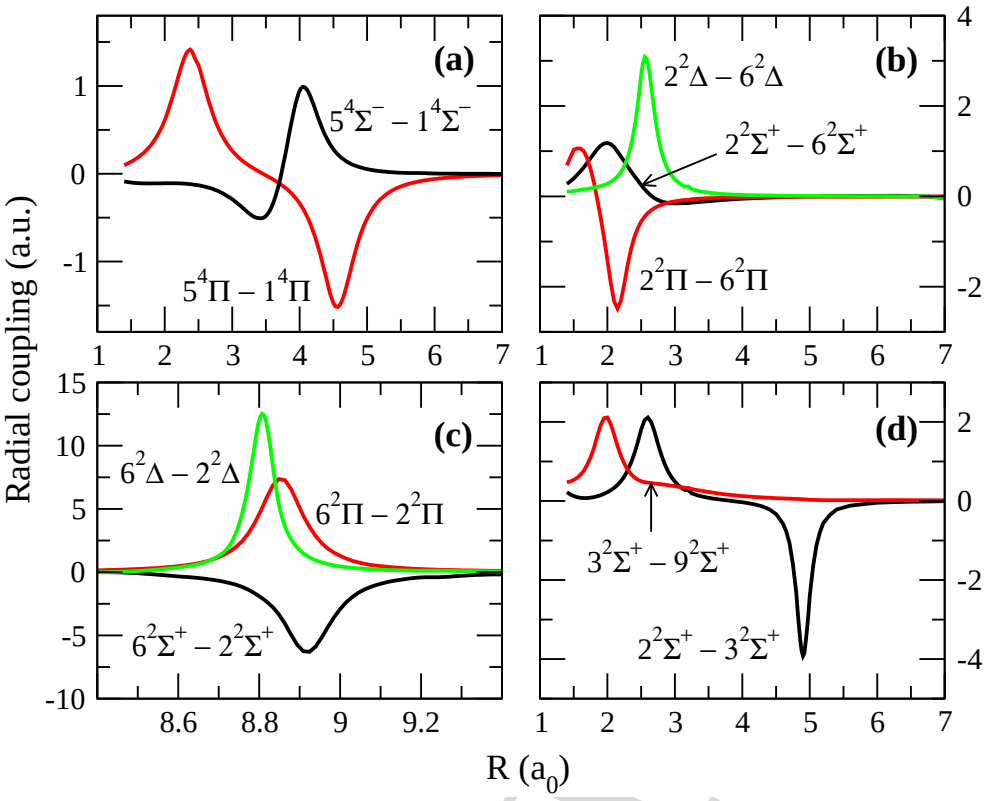

Figure 3. Selected radial couplings between terms of different channels, as indicated in the panels.

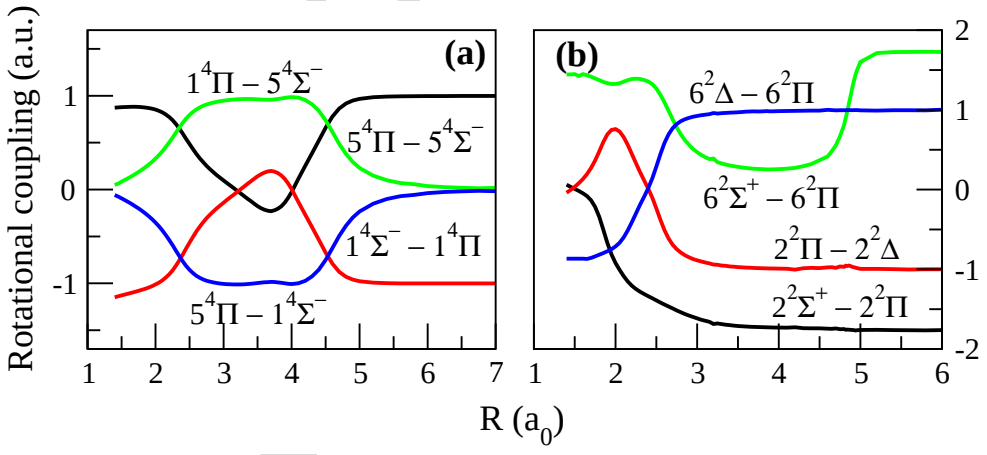

Figure 4. Selected rotational couplings between terms of different channels, as indicated in the panels.

Table 2. Electron capture cross sections (in Å^2) for reactions (1), (2) and (3).

v (a.u.)	(1)	(2)	(3)
0.04	4.66	2.89	6.10
0.06	3.54	2.76	7.46
0.08	4.08	2.87	6.25
0.10	3.70	2.97	5.05
0.12	3.20	3.10	3.83
0.14	2.88	3.20	3.00
0.16	2.57	3.18	2.46
0.18	2.29	3.12	2.13
0.20	2.07	3.04	1.92
0.22	1.91	2.97	1.80
0.24	1.85	2.92	1.72
0.26	1.88	2.87	1.67
0.30	1.98	2.78	1.58
0.35	2.24	2.66	1.48

that can be ascribed to the formation of $O^+(^2D)$ in reaction (2). The total EC cross section for $O^{2+}(^1D)$+H collisions (figure 5) is practically constant because, at relatively high v, the depopulation of individual states through rotational couplings increases the effectiveness of transitions in the avoided crossings $2\{^2\Sigma^+,^2\Pi,^2\Delta\}$–$6\{^2\Sigma^+,^2\Pi,^2\Delta\}$. On the other hand, the EC mechanism in $O^{2+}(^1S)$+H collisions involves, mainly, transitions from the entrance channel ($3^2\Sigma^+$) to states $2^2\Sigma^+$ (and from this to $6^2\Sigma^+$, in last part of the collision) and $9^2\Sigma^+$ (see the corresponding couplings in figure 3d). The $3^2\Sigma^+$–$2^2\Sigma^+$ avoided crossing at $R \simeq 5$ a$_o$ is traversed diabatically when v increases, which explains the decrease of the total cross section for reaction (3) in figure 5. For $E \gtrsim 1$ keV/amu, $3^2\Sigma^+$–$9^2\Sigma^+$ transitions become more important, giving rise to the increase of the partial cross section for formation of $O^+(^2S)$ (see figure 6c).

We obtain good agreement between our theoretical EC cross sections from O^{2+} (^3P) ions with experimental data of Phaneuf *et al* (1982), and worse agreement is found by assuming a contamination of the initial beam by metastable $O^{2+}(^1D)$ or $O^{2+}(^1S)$ ions. Therefore, our results indicate that there was not beam contamination in the experiment of Phaneuf *et al* (1982). In practice, although the order of magnitude of the total cross for reaction (1) of Honvault *et al* (1994) is similar to ours, it does not reproduce the decrease of the experimental cross section for $E \gtrsim 0.45$ keV/amu, because of the limitations of their molecular calculation, and lead them to suggest a high proportion of metastable ions in the initial beam.

5. Conclusions

We have calculated the state selected EC cross sections in collisions of O^{2+} with H(1s), for various initial states of O^{2+}, by employing a molecular expansion with ab initio molecular wavefunctions evaluated with a MRCI technique. The cross sections for EC by

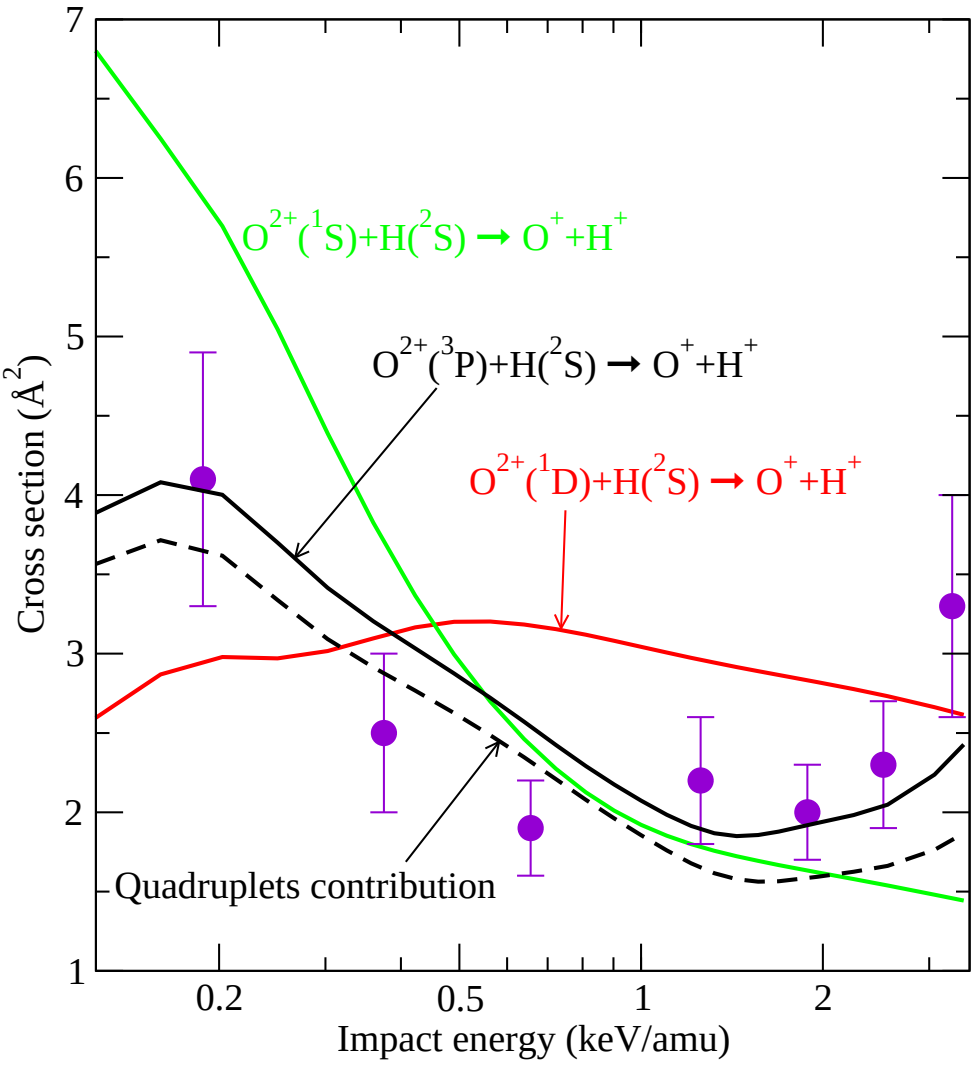

Figure 5. Total electron capture cross sections in O^{2+}+H(1s) collisions from various O^{2+} initial states, as labeled in the figure. In the case of $O^{2+}(^3P)$+H(1s) collisions, the quadruplets contribution is indicated. Symbols are experimental values from (Phaneuf *et al* 1982).

ground state O^{2+} ions are in agreement with previous experimental data of Phaneuf *et al* (1982). We have calculated the branching ratio for populating different EC channels and we show that electron capture with simultaneous projectile excitation is the preferred channel at energies below 1.25 keV/amu, while the direct capture to the 3s orbital of O^+ starts to be competitive at $E \gtrsim 1.25$ keV/amu. O^+ ($2s2p^4\ ^2D$) is practically the only product of capture from $O^{2+}(^1D)$, while O^+ ($2s2p^4\ ^2D$) and O^+ ($2s2p^4\ ^2S$) are obtained from $O^{2+}(^1S)$.

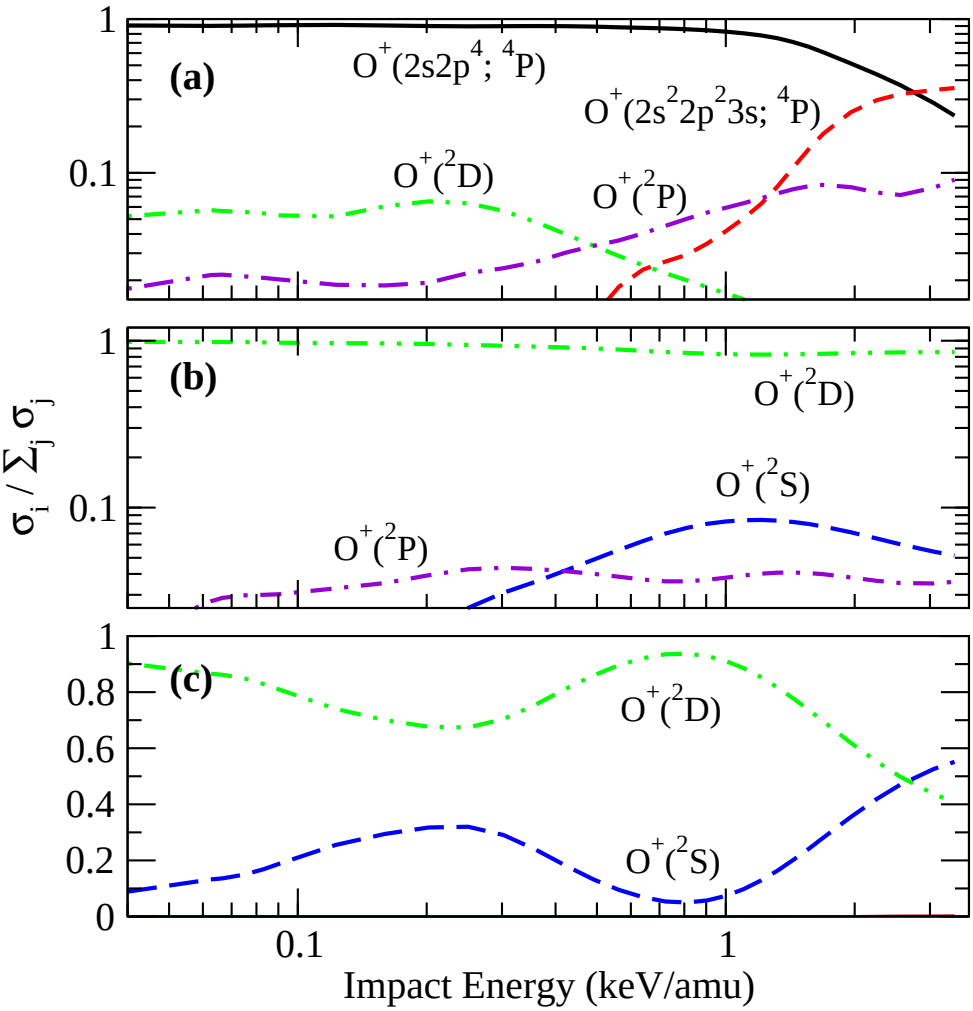

Figure 6. Branching ratio to electron capture channels in O^{2+}+H(1s) collisions. Products are indicated in the panels. Panel (a) is for $O^{2+}(^3P)$+H(1s), panel (b) for $O^{2+}(^1D)$+H(1s) and panel (c) for $O^{2+}(^1S)$+H(1s).

Acknowledgments

IR is grateful to the Spanish MCyT for a "Contrato Ramón y Cajal". This work has been partially supported by DGICYT projects BFM2000-0025 and FTN2000-0911. We thank Dr. Bacchus-Montabonel for helpful discussions and Dr. McCullough for providing us with his unpublished results.

References

Bransden B H and McDowell M H C (1992) *Charge Exchange and the Theory of Ion-Atom Collisions* (Oxford: Clarendon)

Castillo J F, Cooper I L, Errea L F, Méndez L and Riera A 1994 *J. Phys. B: At. Mol. Opt. Phys.* **27** 5011–5026

Castillo J F, Errea L F, Macías A, Méndez L and Riera A 1995 *J. Chem. Phys.* **103** 2113–2116

Davidson E (1990) *in* E Clementi, ed., 'MOTECC, Modern Techniques in Computational Chemistry' ESCOM Publishers B. V., Leiden

Errea L F, Harel C, Jouin H, Méndez L, Pons B and Riera A 1994 *J. Phys. B: At. Mol. Opt. Phys.* **27** 3603

Errea L F, Macías A, Méndez L and Riera A 1999 *J. Phys. B: At. Mol. Opt. Phys.* **32** 4065–4077

Errea L F, Macías A, Méndez L and Riera A 2000*a* *J. Phys. B: At. Mol. Opt. Phys.* **33** 1369

Errea L F, Macías A, Méndez L, Rabadán I and Riera A 2000*b* *J. Phys. B: At. Mol. Opt. Phys.* **33** L615–L621

Errea L F, Méndez L and Riera A 1982 *J. Phys. B: At. Mol. Opt. Phys.* **15** 101

Honvault P, Bacchus-Montabonel M and McCarroll R M 1994 *J. Phys. B: At. Mol. Opt. Phys.* **27** 3115

Leputsch P, Dumitriu D, Aumayr F and Winter H P 1997 *J. Phys. B: At. Mol. Opt. Phys.* **30** 5009–5024

McCullough R W 2000 *Unpublished results*

McLaughlin T K, Wilson S M, McCullough R W and Gilbody H B 1990 *J. Phys. B: At. Mol. Opt. Phys.* **23** 737

Moore C E (1971) *Atomic Energy Levels Nat. Stand. Ref. Data Series vol. 1* (US National Bureau of Standards)

Phaneuf A, Alvarez I, Meyer F W and Crandall D H 1982 *Phys. Rev. A* **26** 1892

Schneiderman S B and Russek A 1969 *Phys. Rev.* **181** 311

Unterreiter E, Schweinzer J and Winter H P 1991 *J. Phys. B: At. Mol. Opt. Phys.* **24** 1003

Voulot D, Gillen D R, Kearns D M, McCullough R W and Gilbody H 2001 *J. Phys. B: At. Mol. Opt. Phys.* **34** 1039

Voulot D, Gillen D R, Thompson W R, Gilbody H B, McCullough R W, Errea L F, Macías A, Méndez L and Riera A 2000 *J. Phys. B: At. Mol. Opt. Phys.* **33** L187–L192

Widmark P O, Malmqvist P and Roos B 1990 *Theor. Chim. Acta* **77** 291